Spectrum Prediction via Graph Structure Learning

Dong Yang, Yue Wang, Zhipeng Cai, and Yingshu Li
Department of Computer Science, Georgia State University, Atlanta, Georgia 30303
Emails: dyang26@student.gsu.edu, {ywang182, zcai, yili}@gsu.edu

***Abstract*—With the rapid development of machine learning technologies, data-driven spectrum prediction enables intelligent dynamic spectrum access to alleviate the bottleneck of spectrum resource scarcity and congestion. However, spectrum prediction still faces some key challenges, including how to exploit the implicit but crucial multi-band correlations in wideband spectrum data, and how to capture the temporal dynamics across different bands. Due to the ignorance of such crucial features inherent from spectrum occupancy patterns, existing learning-based spectrum prediction methods unfortunately suffer from inaccurate prediction performance. To fill this gap, this paper develops a novel model of graph convolutional regression neural network (GCRNN), by introducing efficient graph structure learning (GSL-GCRNN) for dynamic multi-band spectrum prediction. The proposed GSL-GCRNN model is designed to adaptively learn both the multi-band and temporal correlations in dynamic wideband spectrum scenarios. Empowered by the graph structure estimator, graph convolutional networks are fueled to effectively extract the correlations in the frequency domain, followed by gated recurrent unit networks to further extract the temporal correlations of each band. It is worth noting that the graph structure estimator further enables to learn the multi-band correlations across different time periods on-the-fly, enhancing the accuracy of wideband spectrum prediction in dynamic environments. Simulation results verify that our GSL-GCRNN approach outperforms the benchmark methods.**

***Index Terms*—Spectrum prediction, cognitive radio, graph structure learning, graph convolutional network, gated recurrent unit.**

I. Introduction

With the rapid development of wireless communications, an increasing number of spectrum resources are being allocated to various primary user systems. Considering the limited spectrum resources, the scarcity of unallocated spectrum bands becomes a critical bottleneck in the allocation and utilization of spectrum resources. Cognitive radio (CR) [1]–[3], capable of monitoring the target spectrum pool and interacting with the radio environment, is recognized as an effective technology to allow secondary users to detect and access idle spectrum resources. In CR, multi-band spectrum prediction is an enabling technique to obtain the awareness of future spectrum occupancy in wideband sceanrios. It enables CR systems to predict the dynamic spectrum occupancy status and detect the potential spectrum access opportunities for secondary users [4]–[6].

Traditional spectrum prediction methods mainly focus on the temporal domain, but lacking of studies on the frequency domain. Existing works include Markov prediction methods [7], linear regression methods [8], and tensor-based methods [9]. In recent years, deep learning methods have been introduced for spectrum prediction to jointly exploit the potential frequency and temporal correlations. For example, a Long Short-Term Memory (LSTM) model is developed to predict the power spectral density (PSD) values in different frequency ranges and time periods, by jointly exploring the spectral-temporal correlations [10]. In [11], a hierarchical spectrum learning method is developed to perform spectrum availability prediction, by combining a convolutional neural network (CNN) and a recurrent neural network (RNN).

In the real world of wireless communications, there usually exists multi-band correlation between adjacent bands, due to inevitable power leakage from operating band to its adjacent bands [12]. Meanwhile, the multi-band correlation also results from simultaneous spectrum occupancy by the same transmitter over discontinuous bands [13]. Such multi-band correlations can be represented as graph-structured spectrum data, in which the bands and their correlations are expressed as the nodes and edges in the graph. To handle the graph-structured data, graph neural networks (GNNs) are designed to learn the embeddings of the graph nodes, by leveraging the graph topology information [14]. However, existing GNN-based spectrum prediction methods work as a straightforward application of GNNs in traditional traffic prediction fields, while overlooking the widely existed spectrum occupancy patterns [4]–[6]. Considering these inherent patterns, it is crucial to exploit the implicit but important multi-band correlations as well as their temporal dynamics across different bands in spectrum prediction tasks.

To fill the gap, this paper aims at a novel deep learning model of graph convolutional regression neural network (GCRNN), by introducing efficient graph structure learning (GSL-GCRNN) for dynamic multi-band spectrum prediction. In this work, the wideband spectrum data having multi-band correlations is first represented as a graph. Then, a graph structure estimator is proposed to learn the multi-band correlations across different time periods in an on-the-fly mode. In addition, a graph convolutional network (GCN) is used to capture frequency features of spectrum data, while a gated recurrent unit (GRU) learns the temporal features of spectrum changes over time. The main contributions of this work are summarized as follows:

1) To exploit the multi-band correlations and their temporal dynamics stemmed from the inherent spectrum occupancy patterns, this paper formulates the spectrum prediction problem as a graph learning task. To the

This work was supported in part by the National Science Foundation Grants #2146497, #2244219, #2315596, and #2413622.

best of our knowledge, this work is the first attempt to introduce the graph structure learning (GSL) techniques into the GNN-based spectrum prediction, which is capable to adaptively capture the temporal dynamics across different bands.

2) To effectively learn both multi-band and temporal correlations in dynamic wideband spectrum scenarios, we propose the GSL-GCRNN model by integrating three components: GSL, GCN and GRU. For GSL, a graph structure estimator is developed to iteratively update the graph topology information over different time periods. A GCN is applied to capture the frequency features, while a GRU focuses on the temporal features.
3) To evaluate the performance of the proposed GSL-GCRNN approach, we test it compared with different benchmark methods, by using real spectrum data collected from practical sensors. Simulation results reveal that GSL-GCRNN outperforms the existing graph-based methods for spectrum prediction. Our comprehensive experiments demonstrate the merits of GSL-GCRNN thanks to the introduction of GSL into learning-based spectrum prediction.

The rest of this paper is organized as follows. Section II formulates the problem of spectrum prediction. In Section III, the GSL-GCRNN model is proposed through a holistic integration of GCN, GSL, and GRU models. Section IV evaluates the performance of our GSL-GCRNN via comprehensive experiments, followed by the conclusions in Section V.

II. Problem Formulation

Suppose that the wideband spectrum pool is uniformly divided into N bands, where each band can be occupied by primary users (PUs). The wideband spectrum prediction task can be formulated as a multivariate time series prediction task. Its objective is to utilize historical spectrum data monitored by sensors to predict the future spectrum occupancy status. In this work, PSD values are collected as the observed spectrum data for spectrum prediction, recorded in the feature matrix $X = \{x_1, \ldots; x_N\} \in \mathbb{R}^{N\times T}$, where N denotes the number of bands, T represents the number of historical PSD values collected in each band, and x_i with $i = 1, \ldots, N$ is the length-T row vector of X. A graph $G = \{V, E\}$ is used to characterize the frequency correlations between different bands, where the nodes $V = \{v_1, \ldots, v_N\}$ represent the N bands in the spectrum data, and the multi-band correlations are indicated as the edges E in the graph. An undirected graph is utilized to depict the correlations between bands, where the edge $E_{ij} = E_{ji}$ indicates the connection between node i and node j. An adjacency matrix $A \in \mathbb{R}^{N\times N}$ describes the connectivity of edges among the N nodes in the graph. If there exists an edge between node i and node j, then $A_{ij} = 1$, otherwise $A_{ij} = 0$. Meanwhile, the feature matrix X also characterizes the temporal correlations, where X_N^t denotes the length-N column vector of X that contains the features of all the N nodes in the graph at time t.

Thus, the spectrum prediction task boils down to learning a mapping f: $(A, \{X_N^{t-\tau}, X_N^{t-\tau+1}, \ldots, X_N^t\}) \rightarrow \{X_N^{t+1}, X_N^{t+2}, \ldots, X_N^{t+\delta}\}$, where τ represents the number of historical PSD values of N bands, δ represents the number of future PSD values to be predicted, and f is a feature aggregation model composed of trainable model parameters. Learning the mapping f is related to two key factors in the practice of spectrum prediction in wideband scenarios. The first factor arises from power leakage issues, as the energy radiated from radio transmissions in the operating frequency band may extend beyond the assigned bandwidth. Specifically, a PU is transmitting signals at a certain band, which affects the adjacent unoccupied bands due to power leakage. The second factor stems from the multi-band aggregation, where multiple non-contiguous bands can be simultaneously occupied by the same PU. Both factors result in the multi-band correlations.

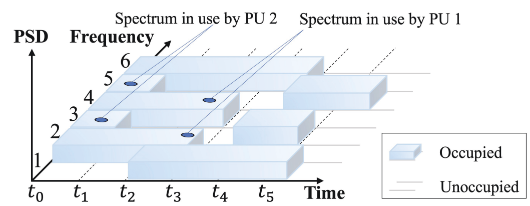

Fig. 1: Dynamic spectrum occupancy in multi-band scenarios.

Moreover, most existing works overlook the multi-band correlations across different time periods. For an illustration, as shown in Figure 1, bands 2 and 4 are simultaneously occupied by PU 1 for transmitting a video stream, and bands 3 and 5 are simultaneously occupied by PU 2 for transmitting text messages. In this way, multi-band correlations caused by simultaneous occupancy exist between bands 2 and 4, and between bands 3 and 5, respectively. As a video stream requires a relatively long transmission time, bands 2 and 4 are simultaneously occupied by PU 1 from time t_0 until time t_3. Meanwhile, bands 3 and 5, used for transmitting text messages by PU 2, have a shorter occupancy time than that by PU 1 for videos. It is worth noting that such multi-band correlations are indeed time-varying. For example, in figure 1, the correlation between bands 3 and 5 is strong from time t_0 to t_1, but becomes weak afterwards. Therefore, it is crucial to consider the multi-band correlations and their temporal dynamics in the design of spectrum prediction model.

III. Proposed Method

To enhance the capability of spectrum prediction and capture the temporal dynamics across different bands, this section proposes a graph-based wideband spectrum prediction model, named GSL-GCRNN, by leveraging the GSL technique.

A. Overview of GSL-GCRNN

We represent the spectrum data in the form of a graph, and propose the GSL-GCRNN model by integrating GCN, GSL and GRU. GCN is utilized to extract frequency domain correlations of spectrum data, and GRU is employed to capture time domain correlations of spectrum data. To better learn

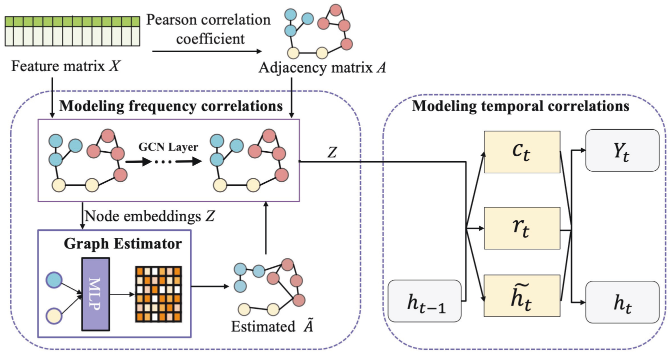

Fig. 2: Framework of the proposed GSL-GCRNN.

the dynamic changes in correlations of spectrum data, a graph structure estimator for GSL is introduced for the first time to extract the multi-band correlations across different time periods on-the-fly. The overall framework of our GSL-GCRNN is illustrated in Figure 2.

B. Graph structure representation

Spectrum data collected over a certain time period records the PSD values of each frequency band at each time point. Feeding such spectrum data, the proposed GSL-GCRNN model in Figure 2 starts with constructing a graph structure. To this end, each frequency band in the spectrum data is treated as a node in the graph. Then, statistical measures such as Pearson correlation coefficient can be used to calculate the correlation between each pair of all frequency bands. Accordingly, the correlation between vectors x_i and x_j, corresponding to the i-th and j-th bands, is measured as:

$$S_{ij} = \frac{\sum_{t=1}^{n}(x_{i,t}-\bar{x}_i)(x_{j,t}-\bar{x}_j)}{\sqrt{\sum_{t=1}^{n}(x_{i,t}-\bar{x}_i)^2\sum_{t=1}^{n}(x_{j,t}-\bar{x}_j)^2}}, \quad (1)$$

where $x_{i,t}$ and $\bar{x}_i$ represent the PSD value of the i-th band at time t and the mean of its all historical PSD values, respectively, and n is the total number of bands.

An adjacency matrix A is then constructed based on the calculated correlation values from (1). Note that the elements in S are continuous-valued and bounded within the interval [0,1], which requires a fully connected graph structure and thus involves substantial computation overhead. Moreover, the most significant correlations typically exist between frequency bands that are either adjacent to or occupied by the same PU. Consequently, a sparse adjacency matrix A is calculated by keeping and binarizing the top k elements from S:

$$A_{ij} = \begin{cases} 1, & \text{if } S_{ij} \in \text{top}k(S_i), \\ 0, & \text{otherwise.} \end{cases} \quad (2)$$

Given all historical spectrum data X, the adjacency matrix A from (2) expresses the statistically significant correlations between bands. Both X and A serve as the inputs to GCN.

C. Graph convolutional network for frequency correlation

Next, GCN is applied to extract the frequency correlation of spectrum data, by following the principle of neighborhood aggregation. Specifically, the feature of each node is updated with the features of its neighbor nodes, whose neighboring relationship is determined by A in (2). This operation is similar to the convolution conducted in convolutional neural networks, but applied under graph structures. For each node, GCN computes the weighted sum of its neighbor nodes' features and its own feature. The neighborhood aggregation at the l-th layer of GCN can be expressed as:

$$Z^l = D^{-1/2}AD^{-1/2}Z^{l-1}W^l, \quad (3)$$

where D is the degree matrix of the symmetric adjacency matrix A, W^l denotes the trainable parameter matrix of the l-th layer, Z^{l-1} represents the input features to the l-th layer, the input to the first layer is $Z^0 = X$, and the output Z^l is the embeddings of the l-th layer.

According to (3), with the fed-in adjacency matrix A and the feature matrix X, the GCN model can be expressed as an input-output manner:

$$Z = \sigma(\text{GCN}(A, X)), \quad (4)$$

where $Z \in \mathbb{R}^{N\times d}$ is the output embeddings of the last layer of the GCN model, d is a hyper parameter denoting the dimensionality of each node embedding row vector, and σ represents the non-linear activation function.

On the one hand, the single-layer operation in (3) shows that each layer of GCN only aggregates the features among the nodes who are one-hop neighbors to each other. On the other hand, the multi-layer operations of the GCN model in (4) enable to capture the potential features between multi-hop nodes via the forward propagation layer-by-layer. In this way, GCN boosts the capability to learn the graphed embeddings among the nodes, corresponding to the frequency correlations between the bands.

D. Graph estimator for graph structure learning

The effectiveness of the aforementioned GCN model relies on the accuracy of the adjacency matrix A provided as the graph structure in (4). In practice, the correlation between bands may change dynamically over time as illustrated in Figure 1. As a result, the original adjacency matrix A calculated via (2) is not able to reflect the time-varying characteristics in the streaming spectrum data. In this sense, the adjacency matrix A needs to be re-estimated on-the-fly to flexibly represent the multi-band correlations and depict the temporal dynamics across different bands. To this end, a graph structure estimator is introduced to re-evaluate the interconnections between node pairs based on the learned node embeddings Z from (4).

Specifically, the embeddings of node v and node u are concatenated and then input into a single-layer feed-forward network to calculate the correlation weight w_{vu} between the two nodes:

$$w_{vu} = [Z_v||Z_u] \cdot W + b, \quad (5)$$

where the operation $||$ concatenates two row vectors to form a double-length row vector, $W \in \mathbb{R}^{2d\times 1}$ is the weighting vector and $b \in \mathbb{R}$ is the bias term. Next, for node $v \in \{1, \ldots, N\}$, the weight w_{vu} from (5) is further regularized over its neighbor nodes to obtain the confidence Q_{vu} on the existence of an edge between node v and node u:

$$Q_{vu} = \frac{\exp(w_{vu})}{\sum_{m\in\mathcal{S}_v} \exp(w_{vm})}, \tag{6}$$

where $\mathcal{S}_v$ represents a set of the top k neighbors of node v, who have the k largest values computed via (5). Thus, the graph structure learned by the graph estimator is formed as $A_Q = \{Q_{vu}, v, u \in \{1, \ldots, N\}\}$. Finally, the estimated adjacency matrix $\tilde{A}$ is updated by combining the original A from (2) with the estimated A_Q as:

$$\tilde{A} = \mu A + (1-\mu)A_Q, \tag{7}$$

where $\mu \in (0, 1)$ is the combination coefficient.

It is worth noting that the adjacency matrix A is used only during the first epoch of GCN training as in (4). Since the second epoch, the estimated adjacency matrix $\tilde{A}$ output from the graph estimator by (7) replaces A in (4), which helps GCN iteratively extract more accurate frequency correlations than by using the original A.

E. Gated recurrent unit for temporal correlation

As an improved version of the LSTM model, the GRU model optimizes the neural network by combining the forget and input gates into a single update gate, resulting in a more efficient network architecture. Compared to the LSTM models, GRU benefits from fewer parameters, faster training speed, and better generalization ability, making it suitable for tasks with small datasets and real-time decision-making requirements. Therefore, we apply the GRU model for capturing temporal correlations of spectrum data.

Given the learned Z from (4) as the input to GRU, a single-layer GRU is adopted as:

$$\begin{aligned} c_t &= \sigma(W_c Z_t + U_c h_{t-1} + b_c), \\ r_t &= \sigma(W_r Z_t + U_r h_{t-1} + b_r), \\ \tilde{h}_t &= \tanh(W_h Z_t + U_h(r_t \odot h_{t-1}) + b_h), \\ h_t &= (1-c_t) \odot \tilde{h}_t + c_t \odot h_{t-1}, \end{aligned} \tag{8}$$

where Z_t denotes the output embeddings of GCN for each frequency band at time t, the function $\tanh(\cdot)$ represents the hyperbolic tangent activation function, c_t and r_t correspond to the update gate and reset gate, respectively, h_{t-1} is the hidden state at time $t-1$, $\tilde{h}_t$ represents the candidate hidden state, the operator $\odot$ denotes element-wise multiplication, h_t indicates the current hidden state, and the parameters $W_c, U_c, b_c, W_r, U_r, b_r, W_h, U_h, b_h$, are all trainable neural weights and biases of the GRU model.

In GSL-GCRNN, the final output $Y_t = \text{MLP}(h_t)$ is obtained by linearly mapping h_t of (8) through a multi-layer perceptron (MLP) network.

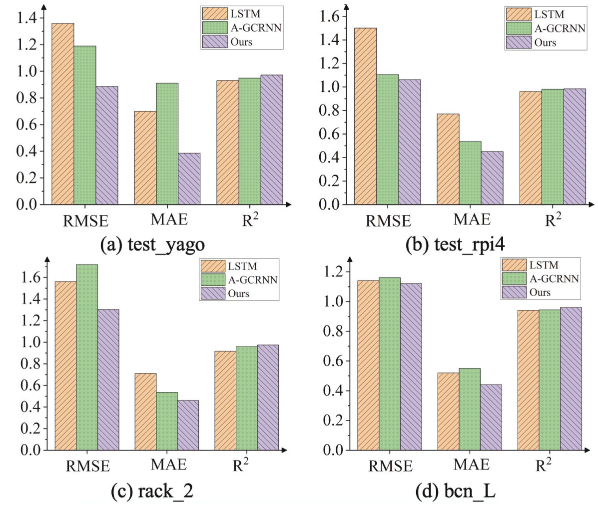

Fig. 3: Prediction results of different methods.

F. Loss function

To train GSL-GCRNN, the mean-square error between the final output Y_t of the model and the ground truth Y_t^* is computed to accurately predict the spectrum state for the future T time steps. The loss function for this task is represented as:

$$L = \frac{1}{T}\sum_{t=1}^{T}(Y_t - Y_t^*)^2, \tag{9}$$

where T denotes the number of future steps, Y_t is the predicted value at time t by GSL-GCRNN, and Y^* is the ground-truth label value.

IV. EXPERIMENTS

In this section, we evaluate the performance of GSL-GCRNN. The baselines used for comparison include LSTM [15] and the existing GNN-based spectrum prediction method A-GCRNN [6].

A. Simulation setup

In this work, we use the dataset collected from the the public platform "Electrosense" [16]. Electrosense is a cloud-based system designed to offer users access to high-quality wireless spectrum data. In our simulations, we collect spectrum measurement datasets from the 600-700 MHz frequency band, measured by four sensors within a 6 km radius in central Madrid, Spain. The four sensors are named: test_yago, test_rpi4, rack_2, and bcn_L. Each dataset spans from June 1st 2021 to June 8th 2021, with a time resolution of 1 minute, resulting in 10,081 time steps. Each dataset covers the 600-700 MHz frequency range with a bandwidth resolution of 2 MHz, thus comprising 101 bands.

In simulations, 80% of the datasets are used as historical data for training, and 20% for testing. The Adam optimizer is applied for training. The time window defined for training the model is 16 steps, meaning that 16 time steps of data are used for training, and the prediction step is defined as 1 step, so each sample contains 17 time steps. The batch size for the

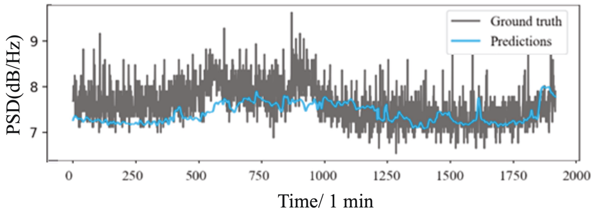

(a) LSTM

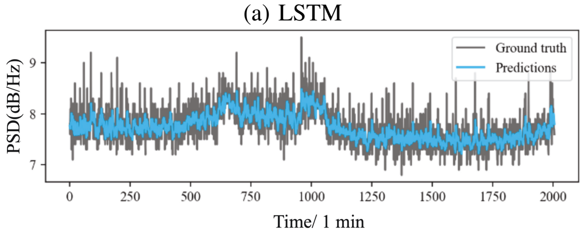

(b) A-GCRNN

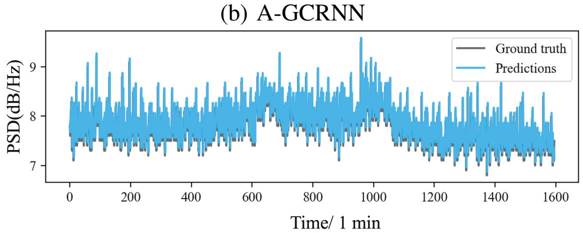

(c) GSL-GCRNN

Fig. 4: Prediction results on test_rpi4 dataset.

proposed model is set to 32, the number of hidden units is set to 64, the number of training epochs is set to 3000, and the learning rate is set to 0.0001.

B. Results and discussion

Root Mean Square Error (RMSE), Mean Absolute Error (MAE), and Coefficient of Determination (R^2) are used to compare the performance of the proposed and baseline models. The simulation results on four datasets are presented in Figure 3, which indicates that GSL-GCRNN always outperforms other benchmark models. It verifies the effectiveness of the proposed GSL-GCRNN in learning the multi-band correlations across different time periods on-the-fly, by improving spectrum prediction performance then other existing methods.

To visualize the spectrum prediction results, we test different modes on the 610 MHz-612 MHz frequency band, selected from the test_rpi4 dataset. In Figure 4, the x-axis represents the time steps within a time interval of 1 minute, and the y-axis represents the PSD of the band. Compared to LSTM and A-GCRNN, the proposed GSL-GCRNN shows superior predictive capability.

V. Conclusion

This paper proposes a novel multi-band spectrum prediction method by leveraging the graph structure learning in the combination with graph neural network and recurrent neural network. As a graph-based approach, we first model the wideband spectrum data as a graph, by treating bands as individual nodes and establishing connections between nodes as links based on multi-band correlations. A new graph structure learning based graph convolutional regression neural network model (GSL-GCRNN) is designed for dynamic learning the inherent correlations in both frequency and temporal domains. In doing so, the frequency band correlations are extracted by a GCN, and then GRU is employed to capture the temporal correlations within each frequency band. It is the graph structure estimator that enables to adaptively learn the multi-band correlation across time periods. In contrast with the latest GNN-based spectrum prediction methods, our GSL-GCRNN model demonstrates its excellent prediction performance.

References

[1] Y. Wang, Z. Tian, and C. Feng, "Sparsity order estimation and its application in compressive spectrum sensing for cognitive radios," *IEEE Transactions on Wireless Communications*, vol. 11, no. 6, pp. 2116–2125, 2012.

[2] ——, "Collecting detection diversity and complexity gains in cooperative spectrum sensing," *IEEE Transactions on Wireless Communications*, vol. 11, no. 8, pp. 2876–2883, 2012.

[3] W. Zhang, Y. Wang, X. Chen, Z. Cai, and Z. Tian, "Spectrum transformer: An attention-based wideband spectrum detector," *IEEE Transactions on Wireless Communications*, pp. 1–11, 2024, Early Access.

[4] H. Zhang, Q. Tian, and Y. Han, "Multi channel spectrum prediction algorithm based on gcn and lstm," in *2022 IEEE 96th Vehicular Technology Conference (VTC2022-Fall)*, 2022, pp. 1–5.

[5] X. Wen, S. Fang, Z. Xu, and H. Liu, "Joint multidimensional pattern for spectrum prediction using gnn," *Sensors*, vol. 23, no. 21, 2023. [Online]. Available: https://www.mdpi.com/1424-8220/23/21/8883

[6] X. Zhang, L. Guo, C. Ben, Y. Peng, Y. Wang, S. Shi, Y. Lin, and G. Gui, "A-GCRNN: Attention graph convolution recurrent neural network for multi-band spectrum prediction," *IEEE Transactions on Vehicular Technology*, vol. 73, no. 2, pp. 2978–2982, 2024.

[7] A. Saad, B. Staehle, and R. Knorr, "Spectrum prediction using hidden markov models for industrial cognitive radio," in *2016 IEEE 12th International Conference on Wireless and Mobile Computing, Networking and Communications (WiMob)*, 2016, pp. 1–7.

[8] S. Geirhofer, L. Tong, and B. M. Sadler, "Cognitive radios for dynamic spectrum access - dynamic spectrum access in the time domain: Modeling and exploiting white space," *IEEE Communications Magazine*, vol. 45, no. 5, pp. 66–72, 2007.

[9] X. Li, Z. Liu, Y. Xu, X. Wang, and T. Song, "Recovering missing values from corrupted historical spectrum observations for dependable spectrum prediction," in *2020 IEEE/CIC International Conference on Communications in China (ICCC)*, 2020, pp. 941–946.

[10] M. A. Aygl, M. Nazzal, M. . Salam, D. B. da Costa, H. F. Ate, and H. Arslan, "Efficient spectrum occupancy prediction exploiting multidimensional correlations through composite 2d-lstm models," *Sensors*, vol. 21, no. 1, 2021.

[11] L. Yu, Y. Guo, Q. Wang, C. Luo, M. Li, W. Liao, and P. Li, "Spectrum availability prediction for cognitive radio communications: A dcg approach," *IEEE Transactions on Cognitive Communications and Networking*, vol. 6, no. 2, pp. 476–485, 2020.

[12] T.-H. Yu, S. Rodriguez-Parera, D. Markovi, and D. abri, "Cognitive radio wideband spectrum sensing using multitap windowing and power detection with threshold adaptation," in *2010 IEEE International Conference on Communications*, 2010, pp. 1–6.

[13] Nidhi, A. Mihovska, and R. Prasad, "Overview of 5g new radio and carrier aggregation: 5g and beyond networks," in *2020 23rd International Symposium on Wireless Personal Multimedia Communications (WPMC)*, 2020, pp. 1–6.

[14] D. Yang, Z. Liu, Y. Wang, J. Xu, W. Yan, and R. Li, "Adaptive multichannel bayesian graph neural network," *Neurocomputing*, vol. 575, p. 127260, 2024.

[15] X. Wang, T. Peng, P. Zuo, and X. Wang, "Spectrum prediction method for ism bands based on lstm," in *2020 5th International Conference on Computer and Communication Systems (ICCCS)*, 2020, pp. 580–584.

[16] S. Rajendran, R. Calvo-Palomino, M. Fuchs, B. Van den Bergh, H. Cordobes, D. Giustiniano, S. Pollin, and V. Lenders, "Electrosense: Open and big spectrum data," *IEEE Communications Magazine*, vol. 56, no. 1, pp. 210–217, 2018.